Experimental Studies about Wave Propagation Properties of Single Layer Lattice Structures —Cantilever Beams and Lattice-Type Plates—

by
Peng Liu, Akemi Nishida and Kenichi Kawaguchi

ABSTRACT

The objective of our research is to examine the wave propagation properties of lattice structures. For the first step of this purpose, we planned and carried out impact hammer experiments on some lattice –type plates. In this paper , firstly, impact experiments performed on cantilever beams with different fixed end which have been carried out as preliminary experiments are reported. Secondly, the experimental results of impact tests performed on lattice-type plates and a continuum plate are shown.

1. Introduction

Spatial structures such as shells, space frames, membrane structures, etc., tend to become larger and lighter recently. For such spatial structures, the investigation and estimation of dynamic structural behavior with respect to earthquake or wind load become an important design factor. The main objective of our research is to investigate the dynamic wave propagtion properties of lattice structures and to use the results for the estimation of structural damping properties of these structures.

In accordance with the first objective, we planned to carry out the impact hammer experiments on some lattice-type plates made of acrylic resin (Photo 1). Each plate was made by cutting away parts from a 3mm thick acrylic plate. A total of four specimens which consist of three types of lattice plate, one continuum plate have been prepared. Before performing the experiments on these plate models, impact response experiments on three types of cantilever beam with different fixed end stiffness were carried out as preliminary experiments with the purpose of obtaining basic data on how to fix the circumferential boundaries of the plate models. The results of preliminary experiments have been used for the design of the table where spacimems were fixed. In this paper, the preliminary experiments on cantilever beams and the impact hammer experiments on lattice-type plates are presented.

2. Preliminary Experiments

2.1 Experimental Method

2.1.1 Experimental Measurement System

Fig.1 shows the experimental measurements system. The same system is used for the experiments on lattice-type plate models. The input force which is a vertical impact force is exerted by using an impact hammer (PCB : GK291C01, Photo 2) and piezoelectric accelerometers (PCB : 352B22) and strain gages (Kyowa : KFP-2-120-C1-65) are used for the purpose of measurement which has been carried out under the following condition: time interval for data sampling = 2μs, total number of sampling = 5000, duration of sampling = 0.1sec and Nyquist frequency = 250kHz. The temperature in the experimental room was 25℃.

2.1.2 Specimens

Fig.2 shows the shapes and dimensions of three cantilever beam specimens used in the experiments. The fixed-end parts of specimen with one, three and five layers are called Type1, Type2 and Type3 respectively. A setup of Type3

is shown in Photo 3. The material used in all specimens is acrylic resin and a special kind of adhesive for acrylic resin is used to bond each layer of fixed-end part. The depth ratios "n" which represent a ratio between the height of fixed-end part and that of beam part for Type1, Type2 and Type3 are 1, 5 and 9 respectivervely. The impact point O, strain measurement positions A_1, A_2, B_1 and B_2, and acceleration measurement position C are shown in Fig.3.

2.1.3 Material Properties

Nominal value was used for mass density of acrylics resin. In order to estimate the Young's modulus, dynamic material test was performed. A square bar with a cross-section of 1cm × 1cm and a length of 50cm which is made from the same acrylic resin is loaded in longitudinal direction by using an impact hammer (Fig.4), and time spent for longitudinal wave to propagate back and forth along the bar is recorded. The time recorded is then used in the calculation of Young's modulus Ed. Fig.5 shows the input acceleration at the impact point of the bar. The impact hammer used in this test is same as the one in other experiments. By using the time lag between two peaks, Young's modulus is calculated. In the calculation, wave velocity of longitudinal wave represented by $c = l/t = \sqrt{Eg/\rho}$ has been used. The material properities are summarized in Table 1. Young's modulus Es which is calculated by using moments obtained in static experiment mentioned in Section2.2.1 is also shown in Table1.

2.2 Experimental Results and Discussions

2.2.1 Static Experiment

Each of the three types of specimen was hung down with a weight of 207.2g at position of 2mm from the free end. The Setup of the static examination is the same as that of the dynamic experiment. After the specimens became the state of repose, the strains of points A_1, A_2, B_1 and B_2 were measured, and the moments of points A and B were obtained. Measurement was performed three times for each type. The obtained moments of point A are shown in Table 2, which the Young's modulus used for calculation is a value of Es. The differences of moments by the thickness of a fixed portion was not observed in this examintion.

2.2.2 Dynamic Experiment

Each of the three types of specimen was struck with the impact hammer four times. Input acceleration at point O, acceleration response at point C and time histories of moment at points A and B are shown in Fig.6(a)-(d) respectively. High frequency responses during the initial part of input acceleration could be confirmed in Fig.6(a). It is conjectured that this is due to the reason that the wave transmits back and forth in the member when the hammer is in contact with the specimen.

Input acceleration at point O and acceleration response at point C are shown overlapping each other in Figure7. From Fig.7(a), it could be seen that after the time when input acceleration becomes zero, the specimen vibrates in free vibration mode. Furthermore, the time lag between the start of input acceleration and that of the acceleration response could be clearly observed in Fig.7(b).

Impedances between moment at point A and input acceleration are calculated for each type. The results are shown in Fig.8. The peak frequencies for each of the three types and the first natural frequency given by classical beam theory (Eular beam theory) are shown in Table 3. Although the peak frequency becomes higer as the depth of the layers of fixed-end parts becomes larger, the difference is expected to have not appeared clearly.

2.3 Discussions of fixed-end part by wave-motion theory

Let us consider wave reflection and transmission at the boundary of two kinds of beam (Fig.9). Displacements in z direction $\hat{w}_1$, $\hat{w}_2$ of each beam are assumed to be given by the following equations:

$$\hat{w}_1 = C_i + C_r = Ae^{-i\beta_1 x} + Ce^{i\beta_1 x} + De^{\beta_1 x} \quad (1)$$

$$\hat{w}_2 = C_t = \overline{A}e^{-i\beta_2 x} + \overline{B}e^{-\beta_2 x} \quad (2)$$

where, $\beta_1 = \sqrt{\omega}(\rho A_1/EI_1)^{\frac{1}{4}}$, $\beta_2 = \sqrt{\omega}(\rho A_2/EI_2)^{\frac{1}{4}}$, and the symbol ^ means that the paramater is transformed by using Fourier transform. The first term on the right-hand side of equation (1) respesents input wave, the second and third term represent reflected wave from the boundary and the two terms on the right-hand side of equation (2) denote transmitted wave. Making use of the equilibrium condition at the discontinuous face and also the continuous condition of displacement, coefficients C, D, $\overline{A}$ and $\overline{B}$ could be expressed as functions of n as shown in Fig.10. It can be seen from Fig.10 that as n increases, coefficients C and D become almost zero, $\overline{A}$ and $\overline{B}$ become almost one. These results show that in the case when n is over the value of 10, the boundary between two beams could be regarded as fixed boundary. In the case of the kind of cantilever beam specimens used in the present study, if the depth of the fixed-end part is more than ten times higher than that of the beam part, the boundary can be assumed as fixed boundary.

2.4 Conclusion remarks of preliminary tests

(1) The results show that the properties of natural frequencies of cantilever beams are not so different in the case of using vises.

(2) For Young's modulas, the dynamic material tests by using impact hammer tend to estimate the value higher than static tests.

(3) Fixed boundary condition lead by wave theory is that fixed-end part have to have over ten times height in comparison with that of a beam section at the boundary in present case.

3. Impact hammer experiments on lattice-type plates

3.1 Experimental Measurement System

Fig.11 shows the experimental measurements system for lattice-type plates models. It is almost the same as that of the preliminary experiments. Only different point is that the measurement system by stain gages is not used. Two piezoelectric accelerometers (PCB : 352B22) are used for the purpose of measurement which has been carried out under the following condition: time interval for data sampling = 2μs, total number of sampling = 20000, duration of sampling = 0.04sec and Nyquist frequency = 250kHz. The temperature in the experimental room was 22-25℃ and there was not big change.

3.2 Specimens

Three types of lattice-type plate and one continuum plate are used in the experiments. The three types of lattice-type plate are called Model1, Model2 and Model3 respectively, and the continuum plate is called Model4. Each lattice-type plates was made by cutting away parts from a 3 mm thick acrylic plate. Diameters of all plates are same, 1200mm, and three lattice-type plates have a circumferential band of 100mm width for boundary. Shape and dimension of cross section of all members consisting of lattice-type plates are same, the height is 3mm and the width is 6mm. The impact point Node1(center point), acceleration measurement positions AC1 and AC2 are shown in Fig.12.

3.3 Experimental Results and Discussion

The center of each specimen was struck with the impact hammer ten times. Force histories at the center point, acceleration responses at points AC1 and AC2 of each model are shown in Figs.13-16 respectively.

3.3.1 Input force histories

(1) The influence of reflected wave

Input force histories at the center point of each model are shown in Figs.13(a),12(a),13(a) and 14(a). The histories during the initial part(4000–4500μs) mainly represent input force by impact hammer. But the responses after 4500μs are disturbed and the time durations are longer in comparison with the responses at points AC1 and AC2 in case of Models 1 and 2. It can be considered that reflected waves from some discontinuities arrived at the impact point during the hammer is in contact with the specimen.

(2) Time duration of responses

It is shown that time duration of force histories of Model 1 and Model 2 are longer than those of Model 3 and Model 4. This is due to the reason that Model 1 and Model 2 have lower stiffness than other models and impact hammer and the specimen move together longer than others.

(3) Wave shapes

Fig.17 shows force histories of all plate models which are divided by each peak value. It is shown that three lattice-type plate models have almost the same properties on the initial wave shapes. The shapes are much different from that of continuum plate. It is considered that this is mainly due to the differences of local stiffness of the models because three lattice-type plate models have same local stiffness at the center.

3.3.2 Acceleration response

(1) Phase

Fig.18 shows acceleration responses at point AC1 of each model. It is shown that the phase of each lattice-type plate model are almost same. The reason is that the phase velocity of lattice-type plates depend on the velocity of flexural wave of the member. Flexural phase velocity of a beam c_{p1} is presented by following formula,

$$c_{p1} = \sqrt[4]{\frac{EI}{\rho A}}\sqrt{\omega} = \sqrt[4]{\frac{Eh^2}{12\rho}}\sqrt{\omega} \tag{3}$$

On the other hand, flexural phase velocity of a plate c_{p2} is shown as following,

$$c_{p2} = \sqrt[4]{\frac{D}{\rho h}}\sqrt{\omega} = \sqrt[4]{\frac{Eh^2}{12(1-\nu^2)\rho}}\sqrt{\omega} \tag{4}$$

The ratio of these velocities is $c_{p1}/c_{p2} = \sqrt[4]{1-\nu^2}$ and it is confirmed from the acceleration responses. The same tendency can be also observed about damping properties of these plates.

(2) Frequency properties

The frequency corresponding to the period that the wave propagates two way in the member is called inner resonance frequency. It is shown that the member distribution density is higher, the number of peaks of the model is more in Fig.19. It seems to be due to the reason that the minimum member length becomes shorter and the variation of member length increases.

3.3.3 Reflected wave from boundaries

High frequency wave propagates faster than low frequency wave in the case of flexural wave of a beam. As the speed of high frequency wave is closer to shear wave velocity of a beam as the frequency becomes higher, it can be assumed that the velocity of head of the pulse is equal to the shear wave velocity of a beam. Using this assumption, the time that reflected wave arrives at the measurement point AC1 can be calculated. The calculated results are shown in Table 4. The figures in brackets represent the time concluded from the data of acceleration responses. The both are well suited.

4. Conclusions

For the purpose of investigation the dynamic wave propagation properties of lattice structures, some lattice-type plates were made by acrylic resin and impact hammer experiments were performed on them. Followings are confirmed from this study.

(1) Wave propagation properties depend on local stiffness of the structures.

(2) Phase and damping properties of lattice-type plates depend on the dynamic properties of a beam and those properties of continuum plate depend on the properties of a plate.

(3) The lattice-type plate Model3 whose minimum member length is shortest has more peaks in frequency domain.

(4) Arrival time of reflected wave obtained according to the assumption that the fastest wave velocity is equal to the phase velocity of shear wave of the beam is agree with the test results.

References

1. Akemi NISHIDA, Peng LIU, Kenichi KAWAKUCHI, Wave Propagation Tests of Single Layer Lattice Structures Part1: Preliminary-Tests, Summaries of Technical Papers of Annual Meeting, Architectural Institute of Japan, C, Structures II, pp.917-918, 1999.

2. Kenshi ODA, A Basic Study of Geometrically Nonlinear Problems in Large-Span and Light-Weight Structures and Their Practical Applications, doctoral thesis, 1994.

3. Seishi YAMADA, Impact Vibration Tests of Lattice Shell Roof Models, Proceedingsof Dynamics, Measurement and Control, Vol.A, The Japan Society of Mechanical Engineers, pp.459-462, 1995.

4. Akemi NISHIDA, Wave Propagation Properties of Large Space Structures – A Study about Wave Propagation Properties of Continuum System and Discrete System -, doctoral thesis, 1993

5. Akio NAGAMATSU, Modal Analysis,Corona, 1993.

6. J. F. Doyle, Wave Propagation in Structure, Springer-Verlag, 1989.

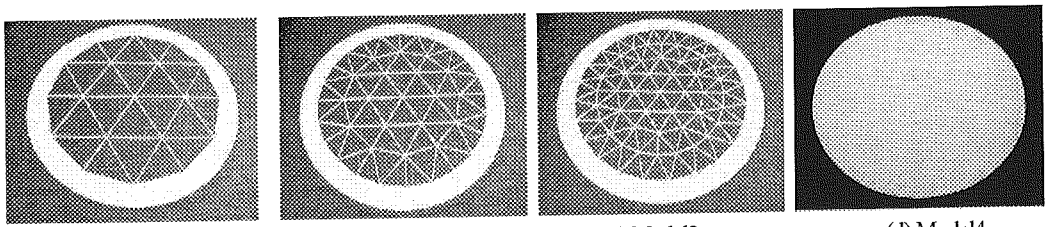

(a) Model1 (b) Model2 (c) Model3 (d) Model4

Photo 1 Lattice-Type Plate Models

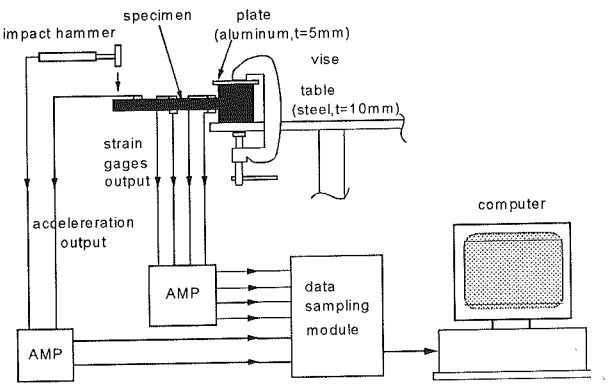

Fig.1 Expermental Measurement System of Preliminary Experiments

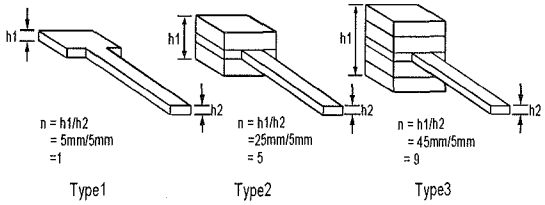

Fig.2 Specimens

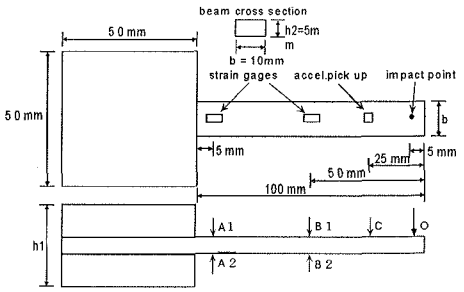

Fig.3 Dimensions and Measurement Positions

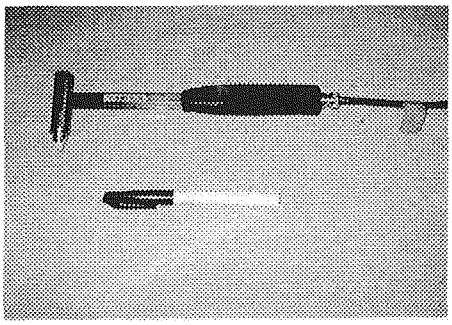

Photo2 An Impact Hammer

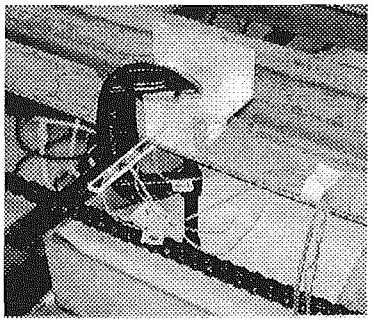

Photo3 Experimental Setup for Type3

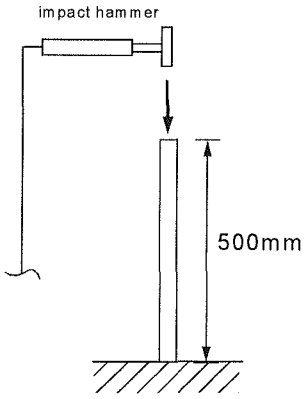

Fig.4 Longitudinal Impact Tests for Young's Modulus

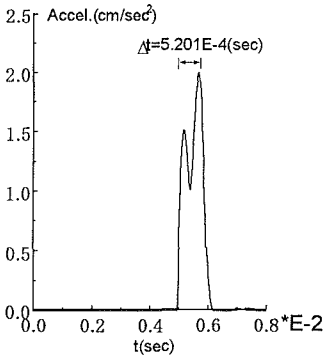

Fig.5 Input Acceleration at the Impact Point

Table 1: Material Properties of Acrylic Resin

Young's Modulus E kg/cm^2	Mass Density ρ kg/cm^3
Es = 3.60×10^4/ Ed = 3.36×10^4	1.19×10^{-3}

Es: static value, Ed: dynamic value

Table 2: The Moment of Point A (kg・cm)

Type1	Type2	Type3	予測値
0.93	0.883	0.905	0.974
(0.955)	(0.907)	(0.929)	(1)

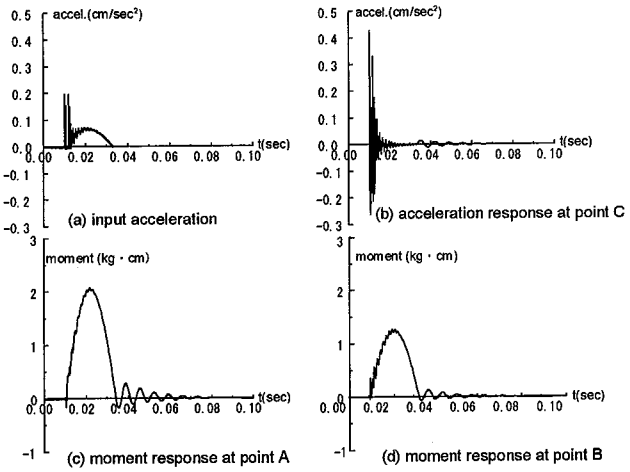

Fig.6 Time Histories of Accelerations and Moments

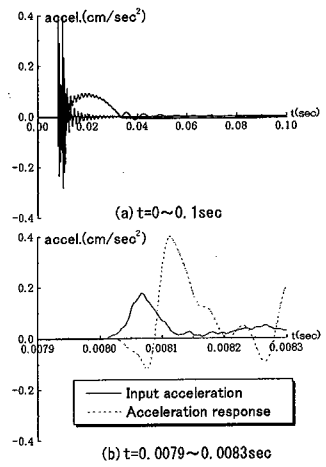

Fig.7 Input acceleration and acceleration response at point C (Type3)

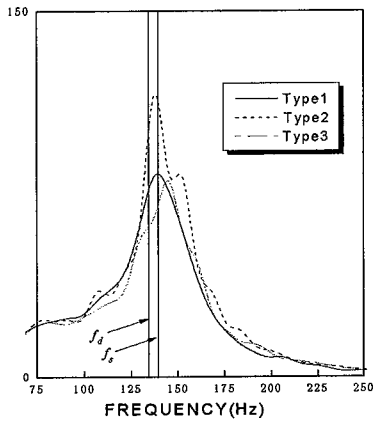

Fig.8 Impedances of Moment at Point A

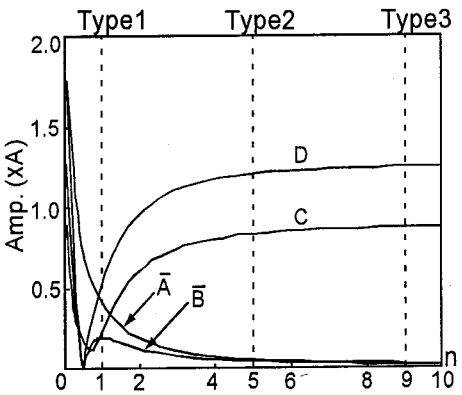

Fig.10 Reflection Coefficients C, D and Transmission Coefficients $\overline{A}$, $\overline{B}$

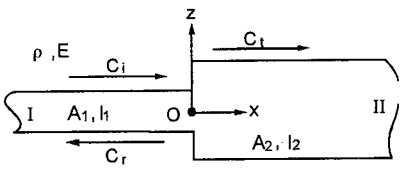

Fig.9 Wave Reflection and Transmission on the Boundary of Two Beams

Table 3 Natural Frequencies (Hz)

Type1	Type2	Type3	Predicted
136.18	137.40	144.37	fd = 134.4 / fs = 139.12

fd: calculated by Ed, fs: calculate by Es

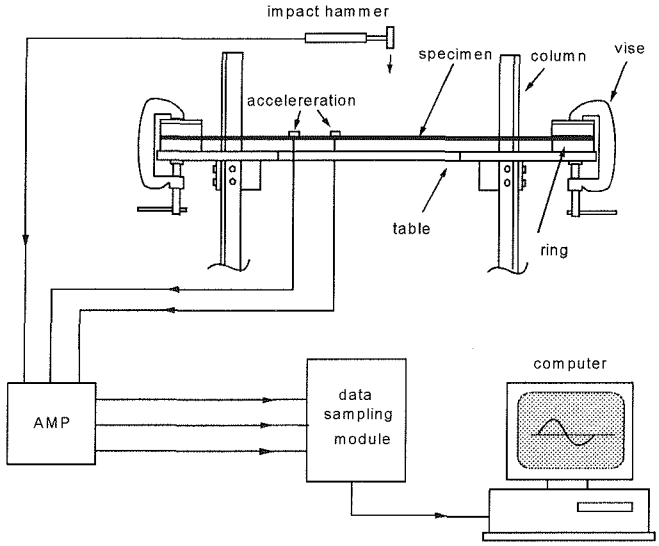

Fig.11 Expermental Measurement System for Lattice-Type Plate Models

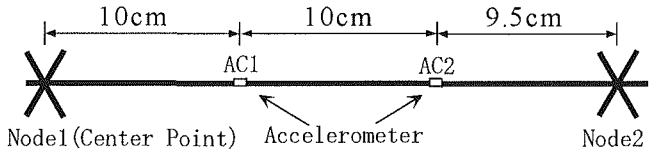

(a) Measurement Positions of Model1

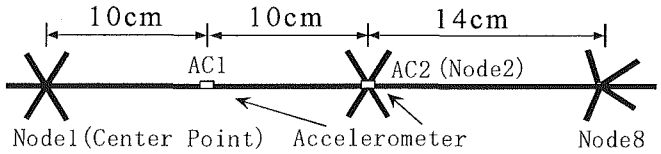

(b) Measurement Positions of Model2

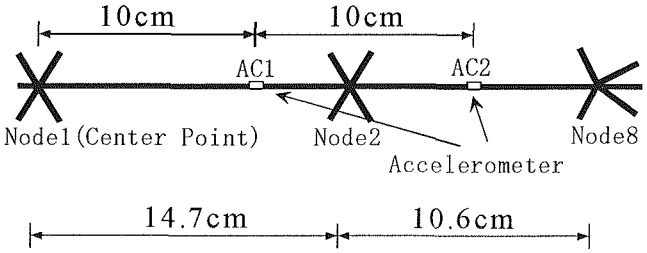

(c) Measurement Positions of Model3

Fig.12 Measurement Positions of Lattice-Type Plate Models

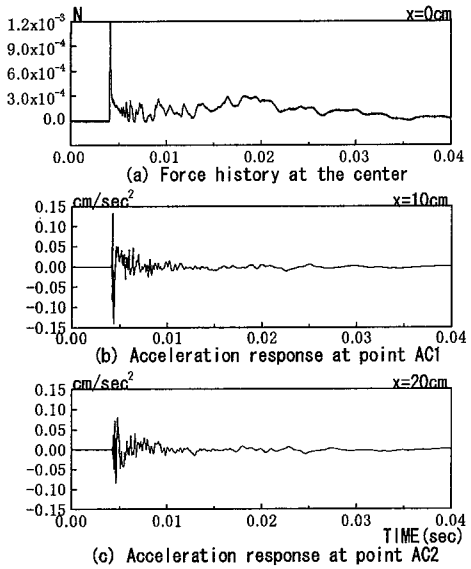

Fig.13 A Typical Case of Responses of Model1

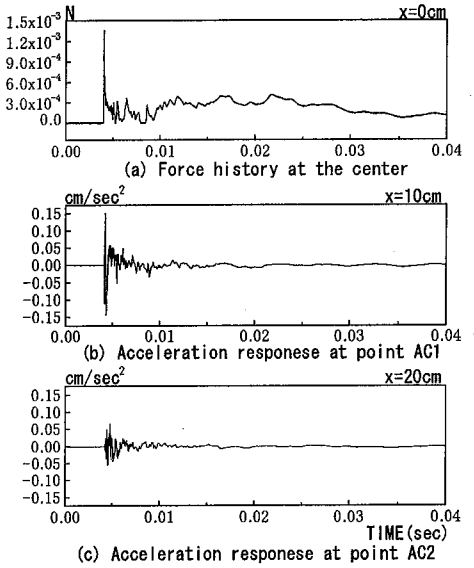

Fig.14 A Typical Case of Responses of Model2

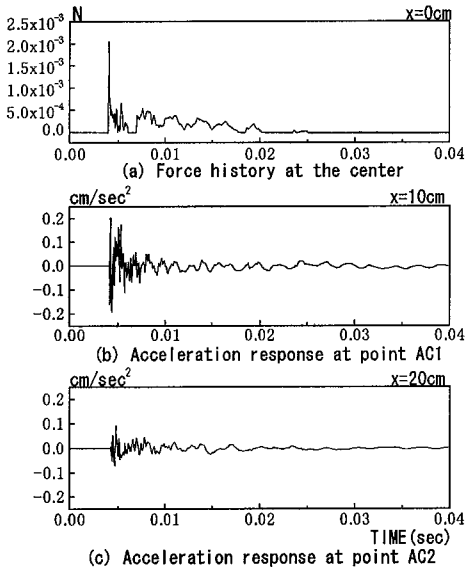

Fig.15 A Typical Case of Responses of Model3

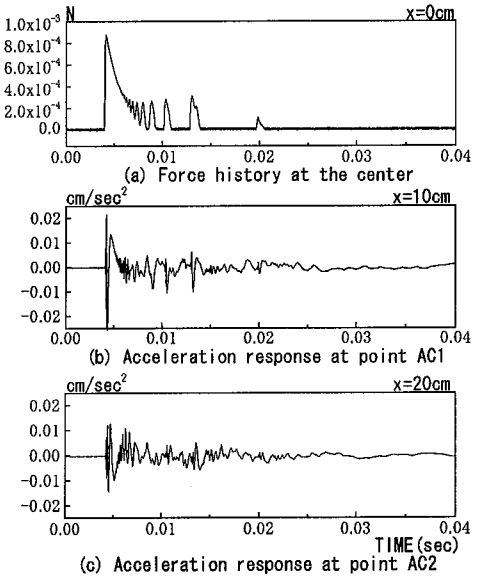

Fig.16 A Typical Case of Responses of Model4

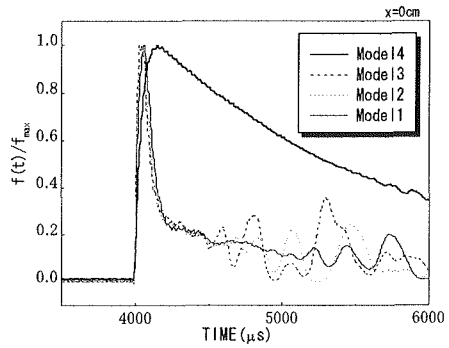

Fig.17 Comparison of Force Histories at the Center

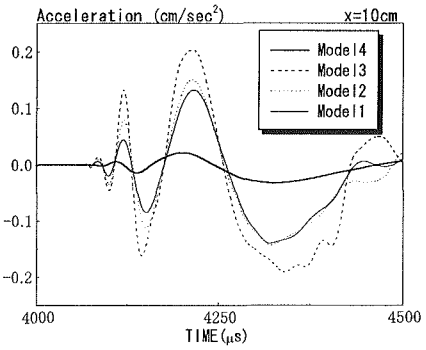

Fig.18 Comparison of Acceleration Responses at Point AC1

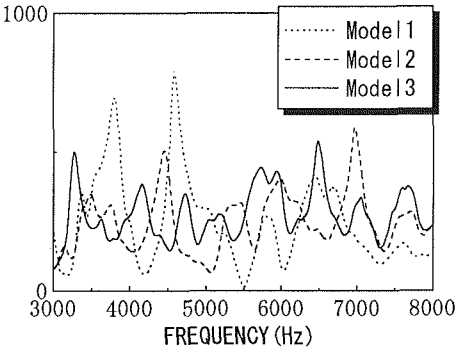

Fig.19 Transfer function of point AC1

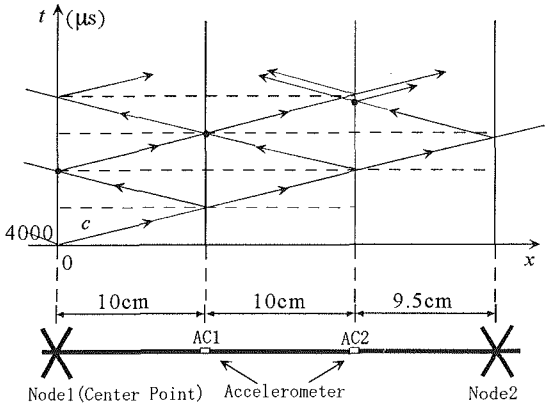

Fig.20 Boundary Reflections and Transmissions of Flexural Waves (Model1)

Table 4 Arrival Time of Reflected Wave (μs)

	Impact Point (Node1)	AC1	AC2
Model1	4208(4220)	4312(4307)	4405(4337)
Model2	4208(4180)	4312(4284)	4416(4386)
Model3	4208(4210)	4202(4261)	4305(4319)
Model4	5040(5300)	4936(4964)	4832(4932)

* Figures in brackets show the time concluded from the experimental results